

## Characteristics of Lignin-based Star Copolymer and Its Application in Soybean Adhesives

Jawad Baley<sup>1</sup>, Yasir Lindblad<sup>1</sup>, Rotich Mylsamy<sup>2</sup>, Markus Sheraz<sup>2,\*</sup>

<sup>1</sup> Uppsala University, Department of Engineering Sciences, Box 534, SE-75121 Uppsala, Sweden

<sup>2</sup> Universidad Autónoma de Nuevo León, Facultad de ingeniería Civil, C. Pedro de Alba s/n, San Nicolas de los Garza, NL, Mexico

\*Corresponding author: m.sheraz@uanl.edu.mx

**Abstract.** Using corn stover lignin as the raw material, a lignin-based chain transfer agent (lignin-CTA) for reversible addition-fragmentation chain transfer (RAFT) polymerization was first synthesized. Subsequently, a lignin star copolymer (lignin-g-PAM) was prepared from lignin-CTA, azobisisobutyronitrile (AIBN), and acrylamide (AM). This copolymer was then separately added to a soy protein isolate (SPI)-water system and a waterborne polyamide-soybean meal flour (SMF)-water system to formulate soy protein-based adhesives and soybean meal-based adhesives, respectively. Various analytical methods were employed to characterize lignin-g-PAM and the resulting adhesives. The research results indicated that lignin-g-PAM was successfully synthesized. The longer the grafted polyacrylamide molecular chains on the lignin, the better the thermal properties and surface activity of the resulting lignin-g-PAM. The copolymer lignin-g-PAM exhibited a significant viscosity-reducing effect on the soy protein-based adhesive, lowered its curing temperature, improved its thermal stability, and disrupted the functional group structures of amide II and III in soy protein. Compared to the soybean meal-based adhesive without lignin-g-PAM, the addition of lignin-g-PAM reduced the apparent viscosity of the soybean meal-based adhesive with a solid content of 44.2% from 10,000 mPa·s to 5,500 mPa·s, improved the toughness of the resulting adhesive layer, and enabled the prepared plywood to meet the wet bonding strength requirements of the national standard for Type II plywood.

**Keywords:** *Lignin copolymer; Amphipathicity; Soybean meal adhesive; Apparent viscosity; High solid content*

Received on 15 Feb 2023, Accepted on 15 April 2023, Published on 15 May 2023

Copyright © 2023 Jawad Baley *et al.* licensed to JGEEEE. This is an open access article distributed under the terms of the CC BY-NC-SA 4.0, which permits copying, redistributing, remixing, transformation, and building upon the material in any medium so long as the original work is properly cited.

### 1 Introduction

The worldwide wood-based panel manufacturing sector, serving as a fundamental pillar for both construction and furniture industries, has historically relied extensively upon formaldehyde-containing thermosetting binders, including urea-formaldehyde (UF), phenol-formaldehyde (PF), and melamine-formaldehyde (MF) resin systems. These petroleum-derived adhesives are favored for their excellent bonding performance, rapid curing, and cost-effectiveness [1]. However, their widespread application carries a significant and persistent burden: the emission of free formaldehyde, a known volatile organic compound (VOC) and human carcinogen, from composite panels throughout their service life [1, 2]. This emission substantially deteriorates indoor atmospheric conditions, presenting significant health hazards encompassing pulmonary irritation, hypersensitive responses, and possible prolonged oncogenic consequences. Consequently, stringent environmental regulations and growing consumer demand for healthier living spaces have propelled the urgent search for high-performance, "formaldehyde-free" adhesive alternatives derived from renewable resources [2, 3].

Soybean-derived products, particularly soy protein isolate (SPI) and soybean meal flour (SMF), have emerged as highly promising candidates for developing eco-friendly wood adhesives [4, 5]. As abundant, renewable, and low-cost agricultural by-products, they offer a sustainable pathway to replace fossil-based resins. Soy proteins are capable of forming cohesive networks through intermolecular interactions, providing the fundamental basis

for adhesion. However, the native soy protein-based adhesives face critical limitations that have hindered their widespread industrial adoption, especially in demanding applications like structural panels [6, 7]. The large molecular weight and the abundance of hydrophilic groups (e.g., -OH, -NH<sub>2</sub>, -COOH) in soy protein lead to inherent drawbacks: poor water resistance and unsatisfactory bonding strength. More critically, from a processing standpoint, conventional soybean adhesives typically suffer from low solid content and high viscosity [8, 9]. A high solid content is crucial for efficient industrial production as it reduces energy consumption during hot-pressing by minimizing the water that needs to be evaporated. Conversely, excessively high apparent viscosity severely impairs the adhesive's workability—it becomes difficult to pump, spread uniformly on wood veneers, and penetrate effectively into wood pores and surface irregularities. This poor processability directly translates to non-uniform glue lines and compromised bonding performance, creating a major technical bottleneck for the commercialization of high-performance soybean adhesives [10].

To overcome these challenges, extensive research has focused on modifying soy protein through physical, chemical, or enzymatic means, or by incorporating reinforcing additives. Among diverse bio-derived additives, lignin—ranking as Earth's second most plentiful natural macromolecule—distinguishes itself through its distinctive aromatic architecture, abundant functional moieties, and accessibility as a principal coproduct from pulp and paper manufacturing operations alongside nascent biorefinery facilities [11]. The polyphenolic architecture of lignin, encompassing abundant reactive functionalities including phenolic and aliphatic hydroxyl moieties, presents opportunities for interaction with soy protein macromolecules. Research has demonstrated that integration of unmodified or minimally modified lignin can augment the adhesive characteristics of soy protein binders via mechanisms encompassing hydrophobic associations, hydrogen bonding, and the establishment of a more extensively cross-linked polymeric network [11]. Furthermore, lignin-based polymers, such as those modified by laccase/TEMPO systems, have been employed to improve specific properties like adhesion performance and fungal resistance [5]. Sodium lignosulfonate has also been used to adjust the properties of soybean meal adhesives [7]. While these approaches demonstrate the potential of lignin, they often do not fundamentally address the core rheological challenges of high viscosity and low solid content. In many cases, simply blending lignin can even exacerbate viscosity issues due to filler effects or poor compatibility.

The application of lignin-grafted copolymers presents a more sophisticated strategy. The pioneering work of Meister et al. [12] early demonstrated the utility of lignin-acrylamide graft copolymers as dispersants in drilling muds. Subsequent research has explored their self-assembly behavior in aqueous solutions and their application as flocculants [13]. These studies underscore the potential of tailoring lignin's properties through graft copolymerization to achieve desired interfacial and solution behaviors. Notably, the amphiphilic nature of such copolymers—with a hydrophobic lignin backbone and hydrophilic polymer grafts—can impart surfactant-like properties, which are precisely the characteristics needed to tackle the viscosity and wettability issues in soybean adhesives. However, the strategic design and application of well-defined lignin-based copolymers, particularly for the purpose of modulating the rheology and enhancing the performance of high-solid-content soybean adhesives, remain a significantly underexplored area. Conventional free-radical grafting often leads to poorly controlled structures. A controlled polymerization methodology is essential for producing lignin-based copolymers exhibiting predetermined structural configurations and performance attributes.

Reversible Addition-Fragmentation Chain Transfer (RAFT) polymerization represents a highly adaptable controlled radical polymerization approach enabling the accurate fabrication of macromolecules with pre-established molecular masses, narrow polydispersity indices, and sophisticated structural designs, encompassing star-shaped configurations when employing multi-functional chain-transfer agents [14, 15]. Applying RAFT to lignin, a naturally branched multifunctional macro-initiator, enables the synthesis of lignin-based star copolymers (lignin-g-Polymer) where multiple polymer arms grow from the lignin core. This architecture can maximize the functional groups introduced per lignin molecule and create a unique amphiphilic structure. Our prior investigation accomplished the successful fabrication of a lignin-derived RAFT chain-transfer agent (lignin-CTA) originating from corn stover lignin [16], thereby establishing the groundwork for accurate vinyl monomer grafting procedures. Acrylamide (AM) is a particularly suitable monomer for this purpose due to its high hydrophilicity, hydrogen-bonding capability, and the ability of polyacrylamide (PAM) chains to interact with both water and the proteinaceous components in soybean adhesives.

Therefore, this study aims to develop a novel, high-solid-content, and low-viscosity soybean adhesive by

incorporating a tailor-made lignin star copolymer. We hypothesize that a lignin-g-polyacrylamide (lignin-g-PAM) copolymer, synthesized via RAFT polymerization, will serve as a multi-functional additive. Its hydrophobic lignin core may interact with the aromatic and hydrophobic regions of soy protein and lignin itself, while the hydrophilic, long-chain PAM arms will compete for water binding, disrupt protein-protein interactions, and provide steric and electrostatic stabilization, thereby dramatically reducing the system's viscosity. Furthermore, the copolymer may participate in the cross-linking network during curing, potentially improving thermal stability and toughness. To test this hypothesis, we first synthesized lignin-g-PAM star copolymers with varying PAM arm lengths from corn stover lignin. The elemental makeup, thermal steadfastness, and interfacial functionalities of the fabricated copolymers were comprehensively scrutinized. Their ramifications on the constitutional chemistry, rheological attributes (manifest viscosity and viscoelastic rebound), solidification patterns, and thermotolerance of a prototypical SPI-engineered adhesive were systematically scrutinized. Consecutively, the optimal copolymer was integrated into constructing a pragmatic SMF-oriented formulation boasting augmented solids fraction. The fabrication characteristics (evident viscosity, residual proportion), the topographical traits of the cured adhesive stratum, and the terminal humidity-defiant bonding efficacy of the fabricated plywood were juxtaposed with a control specimen and archived precedents. This research proffers a pioneering and formidable stratagem for metamorphosing lignin into a superlative adjuvant that surmounts the cardinal fabrication obstacles besetting soy protein adhesives, consequently propelling their ameliorated efficacy and widened mercantile utilization.

## 2 Materials and Methods

### 2.1 Materials and Instruments

Corn stover lignin (industrial grade) was used after methanol purification[16], containing hydroxyl groups 5.18 mmol/g, from Jinan Shengquan Group Co., Ltd. Azobisisobutyronitrile (AIBN, purified by recrystallization), dimethyl sulfoxide (DMSO), NaOH, N,N-dimethylformamide (DMF), pyridine, diethyl ether, dichloromethane, carbon disulfide (CS<sub>2</sub>), 2-bromomethylbutyrate (mass fraction 97%), acrylamide (AM, mass fraction ≥99%), all were analytical grade commercially available. Soy protein isolate (SPI), dispersible type; waterborne polyamide (PAE), solid mass fraction 12.5%±0.5%, pH 4.0~5.0, soybean meal flour (SMF), protein mass fraction 40%~45%, moisture about 1.5%, passed through a 0.096 mm sieve, from Sigma Aldrich.

Nano ZS ZEW 3600 laser particle size analyzer, Malvern Instruments Ltd., UK; Nicolet iS50 Fourier transform infrared spectrometer, Nicolet, USA; HAAK MARSII rotational rheometer, Thermo Fisher Scientific, USA; Bruker DRX 500 nuclear magnetic resonance spectrometer, Bruker, Germany; Sigma701 surface tensiometer, Biolin Scientific, Sweden; STA 409 PC thermogravimetric analyzer, NETZSCH, Germany; DVII+Pro rotational viscometer, Brookfield, USA; XLB flat vulcanizing press, Qingdao Yadong Rubber Machinery Co., Ltd.; CMT4000 universal mechanical testing machine, Shenzhen New Sansi Material Testing Co., Ltd.

### 2.2 Preparation of Lignin Star Copolymer

The lignin star copolymer (Lignin-g-PAM) was prepared according to the method described by Wang Guangbin et al.[16]. 1 g of corn stover lignin, 0.63 g of 50% NaOH solution, and 30 mL of dimethyl sulfoxide were mixed uniformly under ultrasonic oscillation. Then, 1.19 g of carbon disulfide was added under an ice-water bath. Upon completion of 4.5 h equilibration at ambient temperature, 2.91 g 2-bromomethylbutyrate was administered via controlled dropwise introduction, with subsequent agitation sustained for an additional 16 h interval. Following reaction termination, the denser organic phase—recovered through biphasic partitioning with 50 mL n-hexane (×2)—was dispersed into 100 mL purified water, then recovered through centrifugal fractionation. The isolated solid residue was subjected to continuous Soxhlet percolation employing diethyl ether (48 h), then rendered anhydrous under reduced pressure at 40°C to afford the lignin-functionalized RAFT chain-transfer mediator (lignin-CTA). This lignin-CTA, in conjunction with AIBN radical source and AM vinyl monomer, was charged into a hermetically sealed reaction chamber containing 30 mL anhydrous DMF at prescribed molar equivalencies of 3:1:100 and 3:1:500. Following rigorous nitrogen sparging and oxygen scavenging (30 min), the assembly was transferred to a thermoregulated oil bath (50°C) for 36 h polymerization. The crude material was then purified through serial trituration with dichloromethane (2-3 cycles) and vacuum-dried to furnish tan-colored granular products, catalogued as lignin-g-PAM100 and lignin-g-PAM500 commensurate with initial AM stoichiometry.

### 2.3 Preparation of Adhesives

To investigate the interaction between lignin-acrylamide copolymer and soy protein in soybean meal and minimize interference from other factors, the lignin-acrylamide copolymer was first used to modify soy protein. First, 1 g of SPI and 4.5 g of water were weighed, and 0, 0.5, 1, and 2 g of lignin-g-PAM500 were added at room temperature, respectively, and stirred until a uniform consistency was achieved to prepare soy protein-based adhesives, denoted as I, II, III, and IV according to the amount of lignin-g-PAM500 used. Then, 32 g of SMF, 60 g of water, 13.6 g of PAE, and 2.62 g of lignin-g-PAM500 were weighed, stirred until uniform to prepare soybean meal-based adhesive (VI). Keeping other conditions unchanged, a soybean meal-based adhesive (V, without lignin-g-PAM) was prepared as a control by replacing 2.62 g of lignin-g-PAM500 with 2.62 g of SMF.

### 2.4 Preparation of Plywood

The soybean meal-based adhesives prepared in section 1.3 were used to press 3-layer eucalyptus-poplar-eucalyptus plywood. The process parameters were: single-side spread amount 190 g/m<sup>2</sup>, pre-pressing pressure 0.8 MPa, room temperature, cold-pressing time 1 h, hot-pressing pressure 1.0 MPa, temperature 125°C, hot-pressing time 95 s/mm.

### 2.5 Structural Characterization and Performance Testing

#### 2.5.1 FT-IR Analysis

Samples were tested using the infrared spectrometer by attenuated total reflectance method, with 16 scans, resolution 4 cm<sup>-1</sup>, wavenumber range 4000~500 cm<sup>-1</sup>.

#### 2.5.2 <sup>1</sup>H NMR Analysis

Tested using the nuclear magnetic resonance spectrometer, with deuterated dimethyl sulfoxide as solvent, sample concentration 20 g/L, scanning frequency 400 MHz, spectral width 8223 Hz, acquisition time 4.0 s, relaxation time 1.0 s.

#### 2.5.3 TG Analysis

N<sub>2</sub> atmosphere, temperature range 30~900°C, heating rate 10°C/min.

#### 2.5.4 Surface Tension Test

Solutions of different mass concentrations were prepared with deionized water, left standing for 24 h, and then measured with the Sigma701 surface tensiometer at room temperature.

#### 2.5.5 Curing Performance Test

Tested using the HAAK MARS II rotational rheometer under dynamic temperature scanning mode, parallel plate rotor (pp35Ti), test frequency 1 Hz, temperature range 25~200°C, heating rate 5°C/min, gap 1 mm.

#### 2.5.6 Residual Rate Test

Adhesive specimens were equilibrated within a thermostated chamber maintained at 120±2°C until mass stabilization was achieved, subsequently submerged in aqueous medium within a 60±2°C oven for 3 h, then desiccated at 105±2°C for 3 h until mass constancy, whereupon the retention percentage was determined [12].

#### 2.5.7 Apparent Viscosity Analysis

Apparent viscosity was tested using the rotational viscometer.

#### 2.5.8 Crack Observation

Adhesive specimens were uniformly deposited onto glass substrates, thermally set within a 120±2°C chamber for 2 h, transferred to a desiccator, and allowed to equilibrate for 30 min. The solidified adhesive layers were then imaged employing a digital camera equipped with macro optics, with any observable fissures documented.

### 2.5.9 Plywood Performance Test

The prepared plywood was stored at room temperature for 3~4 days. According to the bonding strength analysis method for type II plywood specified, 14 specimens with a lap shear area of 25 mm × 25 mm were immersed in a 63°C water bath for 3 h, then cooled to room temperature. The wet bonding strength was determined using the universal mechanical testing machine at a tensile rate of 5 mm/min.

## 3 Results and Discussion

### 3.1 Structure and Properties of lignin-g-PAM

#### 3.1.1 FT-IR Analysis

The structural composition of the lignin-acrylamide copolymer was examined employing FT-IR spectroscopic methodology, with acquired data depicted in Fig. 1(a). Both lignin-CTA and lignin-g-PAM500 manifest an expansive absorption envelope centered near 3300  $\text{cm}^{-1}$ , originating from O-H stretching vibrations associated with phenolic and aliphatic hydroxyl functionalities. The diagnostic absorptions of lignin-CTA at 1590, 1510, and 1430  $\text{cm}^{-1}$  are indicative of the characteristic phenylpropane skeletal vibrations native to lignin [17]. Regarding the lignin-g-PAM500 spectrum, the band at 3337  $\text{cm}^{-1}$  is assigned to asymmetric stretching of unbound amino groups, the 3190  $\text{cm}^{-1}$  feature corresponds to hydrogen-associated amino stretching, the 2931  $\text{cm}^{-1}$  peak denotes methylene C-H asymmetric stretching, the 1647  $\text{cm}^{-1}$  signal identifies the amide I carbonyl stretching vibration, and the 1410  $\text{cm}^{-1}$  absorption reflects methylene C-H scissoring deformations [18]. The infrared spectrum of lignin-g-PAM500 is quite different from that of lignin-CTA, mainly because in the RAFT polymerization reaction of acrylamide, the proportion of acrylamide is much greater than that of lignin-CTA, so the spectrum of lignin-g-PAM500 is closer to the infrared spectrum of polyacrylamide.

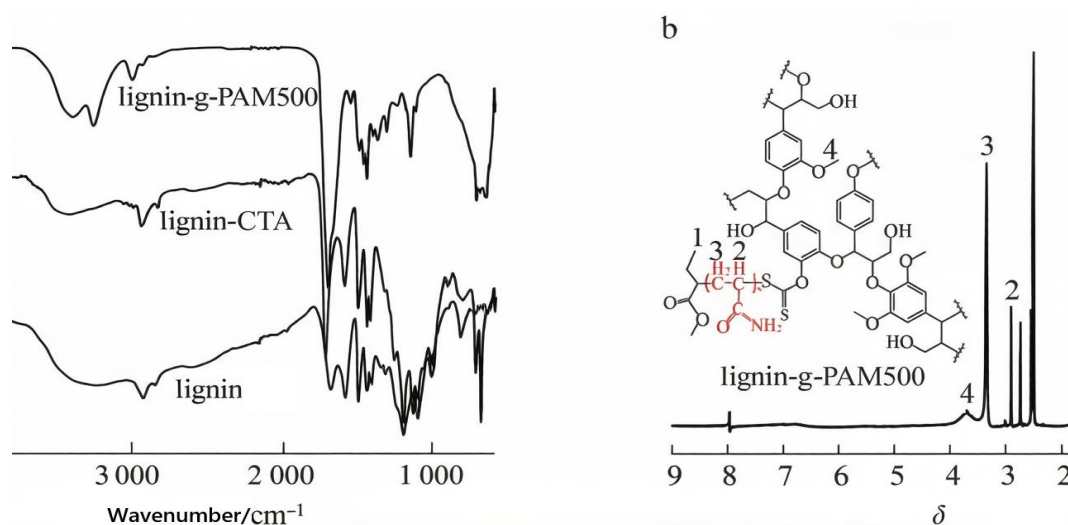


Figure 1 Structural characterization of lignin-g-PAM

#### 3.1.2 $^1\text{H}$ NMR Analysis

To further investigate the structure of the lignin-acrylamide copolymer, its  $^1\text{H}$  NMR spectrum was characterized, and the results are shown in Fig. 1(b). The spectral feature observed at  $\delta$  2.50 is attributable to the residual solvent signal of  $(\text{CD}_3)_2\text{SO}$  [19]. The characteristic peaks at  $\delta$  0.86 and 3.69 are attributed to the active hydrogen proton peaks of the terminal methyl and methoxy groups in lignin-CTA, respectively [20]. The peaks at  $\delta$  2.90 and 3.34 are the hydrogen proton peaks of  $\text{C}_\alpha$  and  $\text{C}_\beta$  in acrylamide. The manifestation of these bifurcated resonances corroborates the assimilation of amide functionalities into the lignin architecture, indicating successful tethering of acrylamide species to the lignin matrix. The pronouncedly superior intensities exhibited by signals 2 and 3 versus signals 1 and 4 establish that the polyacrylamide domain represents the preponderant moiety compared to the native lignin segment within the composite macromolecular entity, validating

congruence with the FT-IR spectroscopic evidence.

### 3.1.3 Thermogravimetric Analysis

Thermogravimetric analysis was employed to evaluate how acrylamide side-chain extension affects the holistic thermal resilience of the graft copolymers, examining unmodified lignin alongside lignin-g-PAM100 and lignin-g-PAM500 derivatives, with degradation profiles illustrated in Fig. 2. It can be seen from the figure that the weight loss process of lignin can be divided into three stages: The first stage ( $40\sim<150^{\circ}\text{C}$ ), the weight loss is mainly related to water evaporation, with a mass loss of 4.5%; The second stage ( $150\sim<260^{\circ}\text{C}$ ), mainly due to the cleavage of aryl ether bonds in lignin[16], dehydration and decarboxylation led to a 7.3% mass loss; The third stage ( $260\sim\leq 540^{\circ}\text{C}$ ), the weight loss is mainly due to C-C cleavage between lignin units and aliphatic side chains of aromatic rings, causing a 36% mass loss.

In the TG-DTG curves of lignin-g-PAM100 and lignin-g-PAM500, the weight loss process also shows three stages. For lignin-g-PAM100, in the range of  $40\sim<165^{\circ}\text{C}$ , the mass loss is 6.1%, attributed to the elimination of water[17]; between  $165\sim<220^{\circ}\text{C}$ , 11.1% of the mass is lost, which is caused by the decomposition of low relative molecular mass polyacrylamide chains generated during the polymerization process[21]. Lignin-g-PAM500 displayed no mass loss event throughout the  $165\sim 220^{\circ}\text{C}$  temperature interval, indicating that extended polyacrylamide chain architectures fortified the copolymer's thermal durability. The 10.4% mass decrement registered for lignin-g-PAM500 beneath  $220^{\circ}\text{C}$  is primarily attributed to aqueous volatilization and thermolytic degradation of short-chain polyacrylamide oligomers [22].the weight loss between  $220\sim 300^{\circ}\text{C}$  is mainly due to the decomposition of high relative molecular mass polyacrylamide chains in the copolymer; the weight loss region after  $300^{\circ}\text{C}$  is mainly due to the decomposition of the lignin skeleton in the sample[22]. The maximum thermal degradation temperatures of lignin-g-PAM100 and lignin-g-PAM500 are  $365^{\circ}\text{C}$  and  $393^{\circ}\text{C}$ , respectively, both higher than the maximum thermal degradation temperature of lignin ( $327^{\circ}\text{C}$ ). This occurrence stems from the selective thermal disintegration of PAM chain segments at comparatively lower temperatures upon heating of the lignin-acrylamide copolymer, which successfully obstructs heat transmission to the lignin core structure [16], consequently bestowing superior thermostability upon the copolymeric framework. When the temperature is below  $220^{\circ}\text{C}$ , the lignin-acrylamide copolymer is stable, and this temperature is much higher than the heating curing temperature of soy protein-based adhesives, so this copolymer can be used as an additive for modifying soybean adhesives.

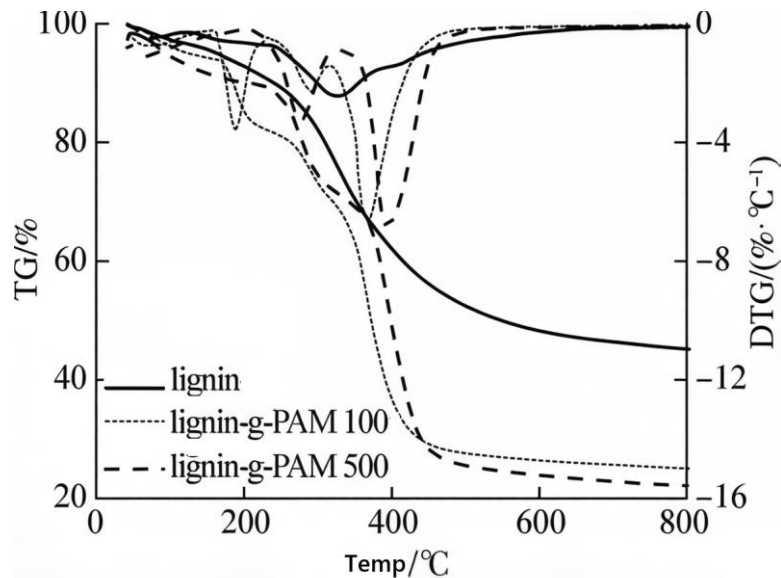


Figure 2 TG-DTG curves of lignin and lignin-g-PAM

### 3.1.4 Surface Activity Analysis

In the lignin-acrylamide copolymer molecule, the lignin backbone part has poor solubility in water, while the

grafted polyacrylamide chains have good solubility in water. The contrasting solubility behaviors of the component segments bestow an amphiphilic character upon the copolymeric structure, thereby furnishing it with native surface-active attributes that facilitate depression of interfacial tension at the air-liquid boundary. The functional relationship between surface tension of lignin-acrylamide copolymer aqueous systems and their mass concentrations within the 20–150 g/L interval is portrayed in Fig. 3. The plotted results demonstrate that an aqueous solution of lignin-g-PAM500 at 20 g/L mass concentration displays a surface tension value of 54.6 mN/m. When its mass concentration is increased to 130 g/L, the surface tension drops to 48.9 mN/m. At this point, the surface tension value of the solution reaches an equilibrium state, and further increasing the copolymer concentration hardly changes the interfacial surface tension. The mass concentration of the solution under this condition is the critical micelle concentration (C<sub>CMC</sub>). As shown in Fig. 3, the C<sub>CMC</sub> value of lignin-g-PAM500 is 70 g/L, and the C<sub>CMC</sub> value of lignin-g-PAM100 is 125 g/L. This indicates that lignin-g-PAM500 has higher surface activity than lignin-g-PAM100. This is attributed to the hydrophobicity of the amphiphilic copolymer molecules and their preferential orientation at the air/water interface[23]. Although the polyacrylamide chain segment in lignin-g-PAM100 is shorter, which helps to increase the hydrophobicity of the molecule, the long chain segment of lignin-g-PAM500 makes its arrangement at the air/water interface more regular, thus giving it a stronger ability to reduce surface tension[23]. Therefore, lignin-g-PAM500 with better surface activity was used for subsequent adhesive modification experiments.

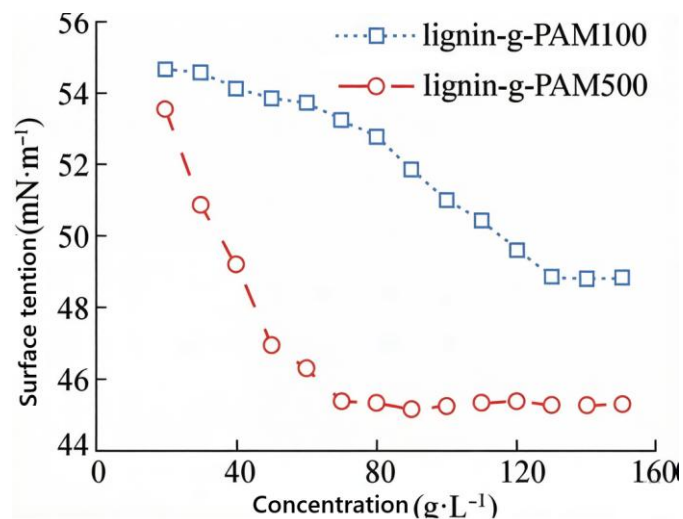


Figure 3 Relationship between surface tension and mass concentration of lignin-g-PAM

### 3.2 Structure and Properties of Soy Protein-based Adhesive

#### 3.2.1 Chemical Structure

To investigate the influence of lignin-acrylamide copolymer on the chemical constitution of soy protein-derived adhesive, FT-IR spectroscopic characterization was conducted on thermally cured soy protein formulations. Soy protein specimens, both with and without lignin-acrylamide copolymer incorporation, were subjected to thermal curing at 120°C for 3 h until complete solidification, followed by analytical evaluation. The resultant spectra are presented in Fig. 4(a). The absorption features at 1632, 1516, and 1234 cm<sup>-1</sup> correspond to the diagnostic amide band vibrations characteristic of soy protein. Specifically, the 1632 cm<sup>-1</sup> band represents carbonyl stretching within amide I, the 1516 cm<sup>-1</sup> band corresponds to N-H bending vibrations within amide II, and the 1234 cm<sup>-1</sup> band signifies C-N stretching vibrations within amide III [18]. Upon lignin-g-PAM copolymer incorporation, the vibrational absorptions at 1516 and 1234 cm<sup>-1</sup> vanish. This observation demonstrates that lignin-g-PAM disrupts the secondary and tertiary amide configurations within the three-dimensional architecture of soy protein, thereby enhancing its chemical reactivity. The TG-DTG thermograms of cured soy protein adhesive (Fig. 4(b)) reveal that sample IV incorporating lignin-g-PAM exhibits an elevated maximum thermal degradation temperature relative to sample I lacking the copolymer. This occurrence presumably stems from hydrogen bonding interactions established between the amide functionalities and lignin segments within lignin-g-PAM macromolecules and the hydroxyl groups present in soy protein, thereby altering the native molecular

organization of soy protein. These structural alterations encompass reinforced intermolecular cohesive forces and the development of a more durable cross-linked polymeric framework [25], ultimately augmenting the thermal resilience of the integrated system.

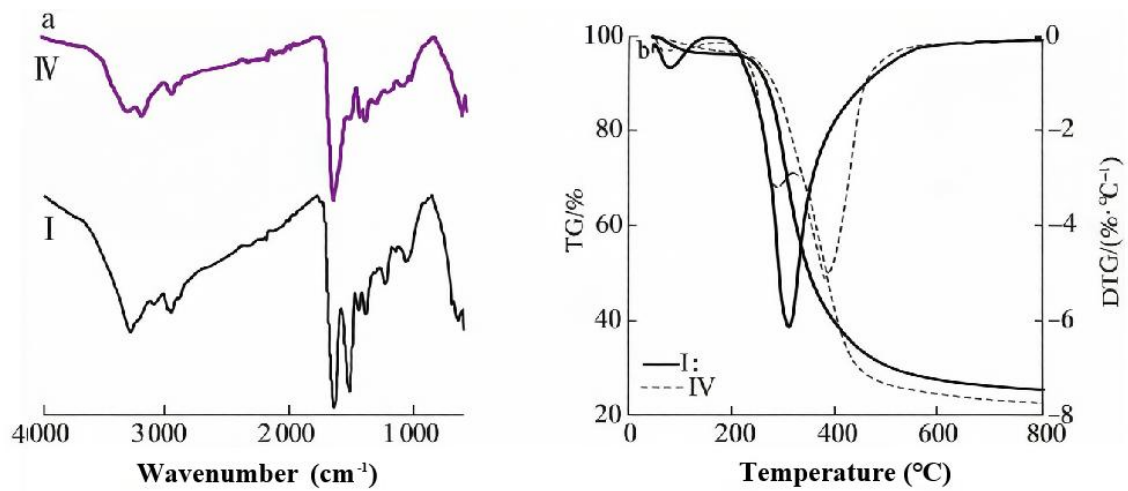


Figure 4 FT-IR spectra(a) and TG-DTG curves(b) of cured soybean protein

### 3.2.2 Viscosity

The viscosity of soy protein-based adhesive with different amounts of lignin-g-PAM500 added as a function of shear rate is shown in Fig. 5. As the shear rate increases, the shear viscosity of the soy protein-based adhesive gradually decreases, showing shear-thinning behavior. Upon attainment of a shear rate approximating  $0.2 \text{ s}^{-1}$ , subsequent elevation of the shear rate fails to intensify the shear-thinning behavior.

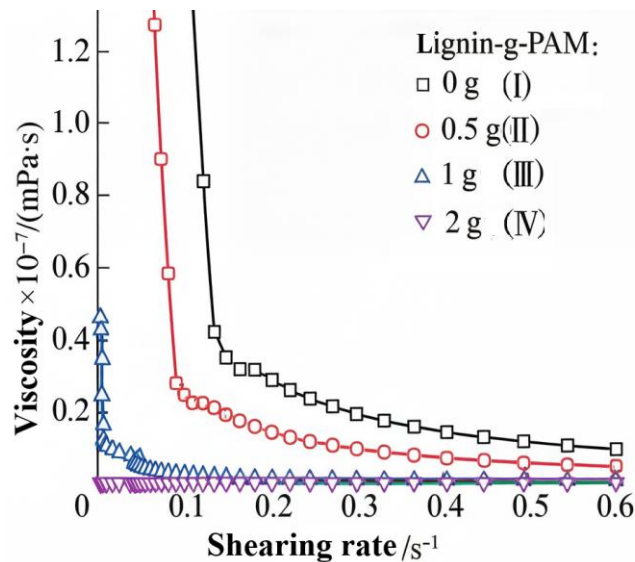


Figure 5 Curves of viscosity versus shear rate for four samples (I-IV)

This is because the orientation or alignment effect of soy protein molecules along the flow direction exceeds the randomization effect of Brownian motion. Upon copolymer incorporation, the zero-shear viscosity of the modified adhesive formulation diminishes. At the same time, a significant decrease in its viscosity can also be clearly seen from the digital photos (Fig. 6). This is because the amphiphilic lignin-acrylamide copolymer has surface activity, and the large number of amino groups in its polyacrylamide chain segment can form hydrogen bonds with water molecules, thus competing with soy protein molecules for binding water molecules. The

aforementioned findings demonstrate that the lignin-acrylamide copolymer enhances the solids loading capacity of soy protein-derived adhesive while concurrently diminishing its apparent viscosity, thereby facilitating superior coating characteristics. This study lays the groundwork for producing low-flow-resistance adhesives derived from soybean meal at high solids loading.



Figure 6 Digital photographs of four samples (I-IV)

### 3.2.3 Curing Viscoelastic Properties

Figure 7 illustrates how incorporating lignin-g-PAM500 modifies the viscoelastic behavior of soy protein adhesive systems. Across the full thermal spectrum from ambient conditions to 200°C,  $G'$  consistently exceeds  $G''$  for all tested specimens. Both  $G'$  and  $G''$  of the unmodified soy protein adhesive (specimen I) exhibit a gradual upward trend with increasing thermal energy. The soy protein-based adhesives with lignin-g-PAM500 added (samples II and III) both show a significant decreasing trend in  $G'$  and  $G''$  at 90°C, speculated to be caused by water evaporation. As shown in Fig. 7(a), the change curves of  $G'$  and  $G''$  with temperature for the soy protein-based adhesive before and after adding the copolymer are not very different. However, after adding the copolymer, its  $G'$  and  $G''$  curves reach an equilibrium state faster with temperature, and the  $G'$  and  $G''$  after reaching equilibrium are lower than before addition.

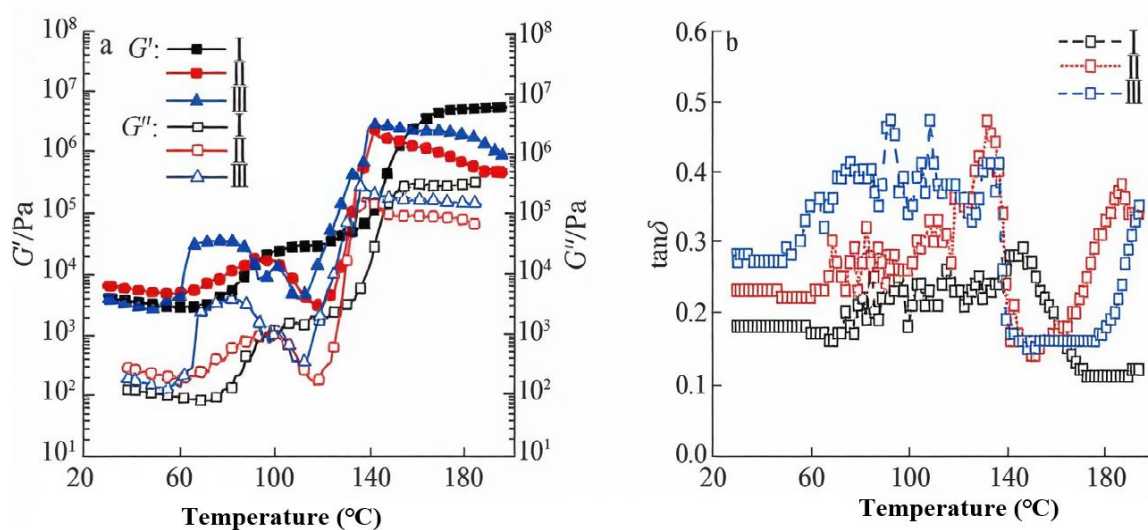


Figure 7 Effect of lignin-g-PAM reagent content on the viscoelastic behavior of soybean-based adhesive

From the change curves of the  $\tan \delta$  value (the ratio of  $G''$  to  $G'$ ) of the soy protein-based adhesive before and after adding the copolymer (Fig. 7(b)), it can be seen that the soy protein-based adhesive with 1 g of lignin-g-PAM added (sample III) overall exhibits a higher viscoelastic response (the highest  $\tan \delta$  value). Before adding the copolymer, the  $\tan \delta$  curve of soy protein (sample I) has a lowest point at 170°C, at which temperature soy protein begins to denature and degrade at high temperature; after adding the copolymer, the  $\tan \delta$  curves of

samples II and III both have lowest points around 140°C, indicating a lower curing temperature. The subsequent elevation in  $\tan \delta$  likely stems from structural alterations in soy protein induced by copolymer incorporation, resulting in the formation of a novel gel network.

### 3.3 Performance of Soybean Meal-based Adhesive

Evaluating fracture patterns enables toughness characterization of waterborne thermoset adhesives[12]; Fig. 8 illustrates how lignin-g-PAM500 modification influences the durability of soy meal-based formulations. Specimen V, lacking copolymer modification, displayed substantial cracking upon curing; conversely, lignin copolymer addition effectively suppressed these imperfections. This phenomenon indicates that the flexible chemical cross-linked network formed between the long acrylamide chains in lignin-g-PAM500 and the PAE rich in active azetidinium groups during heating and curing[26] can increase the toughness of the adhesive layer, helping to balance the internal stress of the plywood[12] and improve adhesion performance.

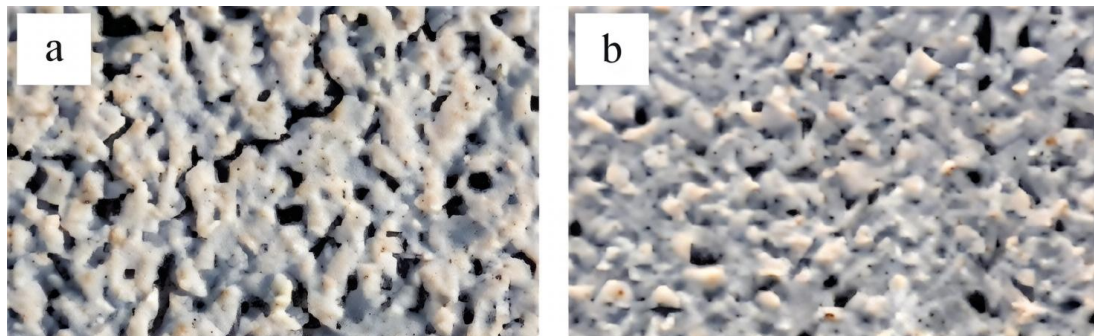


**Figure 8** Observation of cracks in soybean meal-based adhesives

This study assessed flow characteristics and non-volatile content of concentrated soy protein adhesives pre- and post-modification, contextualizing findings within existing research to evaluate scale-up potential. At matched solid concentrations, specimen VI incorporating lignin-g-PAM exhibits markedly inferior flow resistance compared to the control formulation, as data in Table 1 indicate.

**Table 1** Comparison of properties of soybean meal-based adhesives in this work with those in existing literature

Sample	Formulation <sup>1</sup>	Solid Content /%	Apparent Viscosity / (mPa·s)	Residual Rate /%	Reference
V	SMF(34.62 g), H <sub>2</sub> O(60 g), PAE(13.6 g)	44.2	10000	73.3	This work
VI	SMF(32 g), H <sub>2</sub> O(60 g), PAE(13.6 g), lignin-g-PAM500(2.62 g)	44.2	5500	72.9	This work
VII	SMF(28 g), H <sub>2</sub> O(72 g), PHTO(15 g)	28.9	303600	81.9	[27]
VIII	SMF(28 g), H <sub>2</sub> O(72 g), BEP(2 g)	28.3	18400	—	[28]

BEP: bark-based epoxy resin; PHTO: phenol hydroxymethylated tannin oligomers

This is because the added lignin-g-PAM has good surface activity and self-lubricity[29], reducing the mutual friction between molecules in the adhesive. Compared with other systems, this study increased the solid mass fraction of the modified soybean meal-based adhesive while keeping it at a relatively low apparent viscosity, which is conducive to coating and the effective spreading of the adhesive on the surface of wood materials. The residual rate experiment can be used to measure the hydrolysis stability of the adhesive[12]. At 44.2% solid concentration, mass retention of 72.9% for the lignin-g-PAM modified system closely paralleled 73.3% for the

baseline, indicating this copolymer scarcely alters the aqueous degradation resistance of soy meal adhesives.

Wet adhesive strength serves as a critical metric for hydrophobic performance assessment; specimens V and VI registered values of 0.74 MPa and 0.72 MPa under moist conditions, respectively. These findings demonstrate that while lignin-g-PAM addition markedly improves flow characteristics at matched solid concentrations, it marginally compromises the wet shear resistance of bonded wood panels by 2.7%. In the low-viscosity state, sample VI can fully penetrate into wood gaps and be applied more uniformly. At this time, the plywood strength pass rate was 92%, meeting the standard requirements for national Type II plywood (wet bonding strength >0.7 MPa, pass rate >90%).

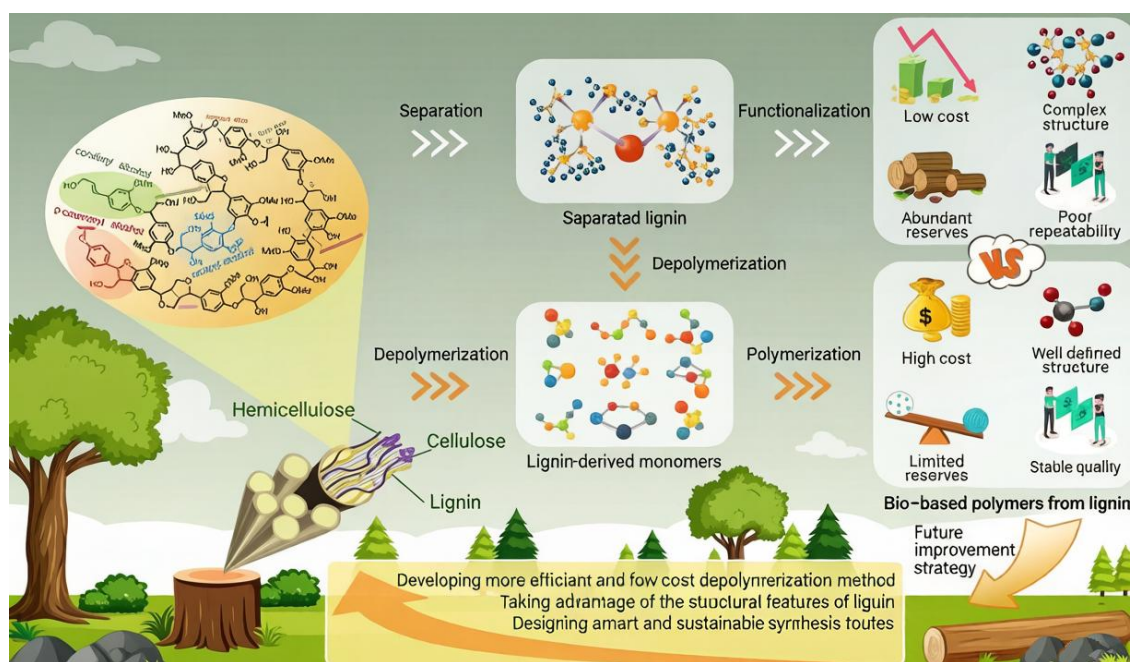


Figure 9 Application of lignin-based biopolymers

Based on the comprehensive experimental data presented in the document, the enhancement mechanism of soybean meal adhesive (SMA) performance by the lignin-g-polyacrylamide star copolymer (lignin-g-PAM) is multifaceted, operating through rheological modification, chemical interaction, and microstructural reinforcement.

The most significant improvement is the dramatic reduction in the adhesive's apparent viscosity, which is the core mechanism enabling high-solid-content formulation. The lignin-g-PAM copolymer acts as a highly effective rheology modifier due to its unique amphiphilic structure. The hydrophilic polyacrylamide (PAM) arms possess a high density of amino groups that compete with soy protein molecules for binding with water molecules via hydrogen bonding. This disrupts the strong protein-protein interactions and the associated entangled network that typically leads to high viscosity in native soy protein systems. Simultaneously, the copolymer exhibits surfactant-like properties, reducing interfacial tension and providing self-lubricity, which decreases molecular friction within the adhesive paste. As a result, the apparent viscosity of the soybean meal-based adhesive with a solid content of 44.2% was reduced from 10,000 mPa·s to 5,500 mPa·s. This lower viscosity drastically improves workability, allowing for more uniform spreading and deeper penetration into wood pores, which is critical for forming a strong mechanical interlock.

Beyond viscosity reduction, the copolymer actively participates in and modifies the chemical and physical structure of the curing adhesive. Spectroscopic analysis revealed that introducing lignin-g-PAM eliminated the signature peaks associated with amide II and III functionalities in the soy protein structure. This indicates the disruption of secondary and tertiary amide structures in the protein's spatial configuration, which increases the protein's reactivity and likely exposes more functional groups for cross-linking. During the hot-pressing cure, a

flexible chemical cross-linked network is formed between the long PAM chains of the copolymer and the reactive azetidinium groups in the co-additive waterborne polyamide (PAE). The interlocking polymer architecture enhances the ductility of the hardened adhesive film, as demonstrated by the marked attenuation of cracking compared to the brittle reference sample. Secondary bonding between amide/lignin functionalities on the graft copolymer and hydroxyl sites of the protein backbone reinforces the cross-linked framework, yielding superior heat resistance as validated by TGA profiles. In summary, the performance enhancement is not due to a single factor but a synergy of mechanisms: the amphiphilic copolymer acts as an internal lubricant and water-competitor to enable high-solids processing, a chemical modifier to increase protein reactivity, and a co-cross-linker to form a tougher, more thermally stable adhesive network. While the wet bonding strength saw a marginal decrease (from 0.74 MPa to 0.72 MPa), the vastly improved processability and the achievement of a satisfactory strength meeting the Type II plywood standard ( $> 0.7$  MPa) with a 92% pass rate demonstrate the overall success of this modification strategy.

## 4 Conclusion

A RAFT chain transfer agent was initially fabricated from corn stover lignin, followed by the preparation of a lignin-centered star copolymer (lignin-g-PAM) through free radical polymerization of acrylamide initiated by AIBN. FT-IR and  $^1\text{H}$  NMR analysis confirmed the successful synthesis of lignin-g-PAM. Thermogravimetric analysis and surface activity test results showed that lignin-g-PAM with longer grafted acrylamide chains has better thermal stability and surface activity. The maximum thermal degradation temperature of copolymer lignin-g-PAM500 is  $393^\circ\text{C}$ , and it is not easy to decompose at the curing temperature of the modified adhesive; its critical micelle concentration ( $C_{\text{CMC}}$ ) value is 70 g/L, and it can achieve a good viscosity reduction effect at a relatively low addition amount.

Lignin-g-PAM500 integration induced structural perturbations in the amide II and III domains of soy protein, simultaneously reducing pre-cure viscosity and curing activation energy whilst elevating thermal stability of the resulting binder. At 44.2% solid loading, the engineered soy protein binder (specimen VI) demonstrated a substantially diminished flow resistance of just 5500 mPa·s. Compared with other literature studies, the solid mass fraction of this system is significantly increased and the viscosity is low, and the resulting plywood still meets the standard requirements for national Type II plywood.

## References

- [1] SOLT P, KONNERTH J, GINDL-ALTMUTTER W, et al. Technological performance of formaldehyde-free adhesive alternatives for particleboard industry[J]. *International Journal of Adhesion and Adhesives*, 2019, 94: 99-131.
- [2] KUMAR R, CHOUDHARY V, MISHRA S, et al. Adhesives and plastics based on soy protein products[J]. *Industrial Crops and Products*, 2002, 16(3): 155-172.
- [3] HEINRICH L A. Future opportunities for bio-based adhesives-advantages beyond renewability[J]. *Green Chemistry*, 2019, 21(8): 1866-1888.
- [4] PRADYAWONG S, QI G, LI N, et al. Adhesion properties of soy protein adhesives enhanced by biomass lignin[J]. *International Journal of Adhesion and Adhesives*, 2017, 75: 66-73.
- [5] XIAO Z G, LI Y H, WU X R, et al. Utilization of sorghum lignin to improve adhesion strength of soy protein adhesives on wood veneer[J]. *Industrial Crops and Products*, 2013, 50: 501-509.
- [6] PRADYAWONG S, QI G Y, SUN X S, et al. Laccase/TEMPO-modified lignin improved soy-protein-based adhesives: Adhesion performance and properties[J]. *International Journal of Adhesion and Adhesives*, 2019, 91: 116-122.
- [7] IBRAHIM V, MAMO G, GUSTAFSSON P J, et al. Production and properties of adhesives formulated from laccase modified kraft lignin[J]. *Industrial Crops and Products*, 2013, 45: 343-348.
- [8] LI Ning, GU Limin, WANG Chunpeng, et al. Effects of different sodium lignosulfonate on the properties of soybean meal adhesives[J]. *Fine Chemicals*, 2021, 38(1): 206-211.
- [9] CHEN S Q, CHEN H, YANG S, et al. Developing an antifungal and high-strength soy protein-based adhesive modified by lignin-based polymer[J/OL]. *Industrial Crops and Products*, 2021, 170: 113795[2024-08-10]. <https://doi.org/10.1016/j.indcrop.2021.113795>.

- [10] ZHANG X C, ZHU Y D, YU Y M, et al. Improve performance of soy flour-based adhesive with a lignin-based resin[J/OL]. *Polymers*, 2017, 9(7): 261[2024-08-10]. <https://doi.org/10.3390/polym9070261>.
- [11] GUI C S, LIU X Q, WU D, et al. Preparation of a new type of polyamidoamine and its application for soy flour-based adhesives[J]. *Journal of the American Oil Chemists' Society*, 2012, 90(2): 265-272.
- [12] ZHANG Y, ZHANG M, CHEN M S, et al. Preparation and characterization of a soy protein-based high-performance adhesive with a hyperbranched cross-linked structure[J]. *Chemical Engineering Journal*, 2018, 354: 1032-1041.
- [13] MEISTER J J, PATIL D R, CHANNELL H. Properties and applications of lignin-acrylamide graft copolymer[J]. *Journal of Applied Polymer Science*, 1984, 29(11): 3457-3477.
- [14] HASAN A, FATEHI P. Self-assembly of kraft lignin-acrylamide polymers[J]. *Colloids and Surfaces A: Physicochemical and Engineering Aspects*, 2019, 572: 230-236.
- [15] ALDAJANI M, ALIPOORMAZANDARANI N, KONG F, et al. Acid hydrolysis of kraft lignin-acrylamide polymer to improve its flocculation affinity[J/OL]. *Separation and Purification Technology*, 2021, 258: 117964[2020-11-13]. <https://doi.org/10.1016/j.seppur.2020.117964>.
- [16] WANG Guangbin, CHEN Jiabao, GU Limin, et al. Synthesis and characterization of lignin based chain transfer agent used for RAFT polymerization[J]. *Chemistry and Industry of Forest Products*, 2018, 38(6): 75-80. (in Chinese)
- [17] WANG S J, SUN Y Y, KONG F G, et al. Preparation and characterization of lignin-acrylamide copolymer as a paper strength additive[J]. *BioResources*, 2016, 11(1): 1765-1783.
- [18] CHEN Hesheng, SHAO Jingchang. Analysis of polyacrylamide by infrared spectroscopy[J]. *Analytical Instrumentation*, 2011(3): 50-54. (in Chinese)
- [19] FULMER G R, MILLER A J M, SHERDEN N H, et al. NMR chemical shifts of trace impurities: Common laboratory solvents, organics, and gases in deuterated solvents relevant to the organometallic chemist[J]. *Organometallics*, 2010, 29(9): 2176-2179.
- [20] SUN Yan, LIU Hewen. Functionalization of  $\beta$ -cyclodextrin via  $\beta$ -cyclodextrin xanthate mediated RAFT polymerization[J]. *Journal of Functional Polymers*, 2009, 22(3): 282-288. (in Chinese)
- [21] SAHOO P K, MOHAPATRA R, SAHOO A, et al. Characterization, biodegradation, and water absorbency of chemically modified tossa variety jute fiber via pulping and grafting with acrylamide[J]. *International Journal of Polymer Analysis and Characterization*, 2005, 10(3/4): 153-167.
- [22] DOMÍNGUEZ J C, OLIET M, ALONSO M V, et al. Thermal stability and pyrolysis kinetics of organosolv lignins obtained from eucalyptus globulus[J]. *Industrial Crops and Products*, 2008, 27(2): 150-156.
- [23] ZHOU M S, WANG W L, YANG D J, et al. Preparation of a new lignin-based anionic/cationic surfactant and its solution behaviour[J]. *RSC Advances*, 2015, 5(4): 2441-2448.
- [24] ALWADANI N, GHAVIDEL N, FATEHI P. Surface and interface characteristics of hydrophobic lignin derivatives in solvents and films[J/OL]. *Colloids and Surfaces A: Physicochemical and Engineering Aspects*, 2021, 609: 125656[2020-10-15]. <https://doi.org/10.1016/j.colsurfa.2020.125656>.
- [25] LI Ning, LIU Jingyi, WANG Chunpeng, et al. Preparation and properties of soybean meal adhesives modified by lignin amine[J]. *Biomass Chemical Engineering*, 2022, 56(3): 23-28.
- [26] SUN Zongxing, YE Renwei, JIAN Jianlin, et al. Effect of pH of PAE resin on the structure and properties of soybean adhesive[J]. *Journal of Forestry Engineering*, 2021, 6(6): 130-136.
- [27] CHEN M S, ZHANG Y, LI Y, et al. Soybean meal-based wood adhesive enhanced by phenol hydroxymethylated tannin oligomer for exterior use[J/OL]. *Polymers*, 2020, 12(4): 758[2020-11-13]. <https://doi.org/10.3390/polym12040758>.
- [28] LUO J, ZHOU Y, GAO Q, et al. From wastes to functions: A new soybean meal and bark-based adhesive[J]. *ACS Sustainable Chemistry & Engineering*, 2020, 8(29): 10767-10773.
- [29] ZAHRAN M A, EL-SHERBINY I M, ABD EL-RAHEEM H M, et al. Synthesis, characterization and aqueous properties of a newly prepared lignin-based graft copolymer as a drilling mud additive[J]. *International Journal of Thin Films Science and Technology*, 2017, 6(1): 1-7.